Enzymatic Modification of Self-Assembled Peptide Structures with Tissue Transglutaminase

ARTICLE *in* BIOCONJUGATE CHEMISTRY · JULY 2003

Impact Factor: 4.51 · DOI: 10.1021/bc034017t · Source: PubMed

2 AUTHORS, INCLUDING:

Joel Collier
University of Chicago
41 PUBLICATIONS **1,830** CITATIONS

SEE PROFILE

Enzymatic Modification of Self-Assembled Peptide Structures with Tissue Transglutaminase

Joel H. Collier and Phillip B. Messersmith*

Northwestern University, Department of Biomedical Engineering, 2145 Sheridan Road, Room E310, Evanston, Illinois 60208 Received February 11, 2003; Revised Manuscript Received May 15, 2003

A de novo peptide that self-assembles into fibrillar structures and serves as a substrate for the cross-linking enzyme tissue transglutaminase was developed (Ac-QQKFQFQFEQQ-Am). Congo red staining, circular dichroism, and FTIR spectroscopy showed that this 11-amino acid peptide produced predominantly β-sheet structures. TEM with negative staining and quick-freeze deep etch (QFDE) TEM showed that the peptide structures were composed of a highly entangled fibrillar network. These β-sheet fibrillar nanostructures were then covalently coupled to pendant amine-containing biomolecules via tissue transglutaminase. MALDI-TOF mass spectrometry and HPLC were utilized to monitor the extent of the transglutaminase modification of the peptide, showing that as many as five glutamines in the peptide were reactive via transglutaminase for covalent conjugation. This strategy, based on the post-assembly modification of a self-assembling peptide, has potential applications for tailoring supramolecular structures for drug delivery, tissue engineering, or other biomedical applications.

INTRODUCTION

Self-assembling systems based on peptides, lipids, or hybrid peptide−amphiphiles are currently being investigated as potential materials for biomedical applications such as controlled drug release matrixes and tissue engineering scaffolds (*1*−*7*). In these approaches, small molecules are designed such that they self-assemble into complex nanostructures, in many cases fibrillar networks or hydrogels. The assembly of these materials is highly dependent on solution conditions such as pH, temperature, solvent polarity, and the presence of salts. Because of this sensitivity to solution conditions, self-assembly can often be induced with small, physiologically benign perturbations of pH, salt content, or temperature, making these materials attractive candidates for new in situ gelling biomaterials (*7*, *8*). Peptides are particularly attractive self-assembling molecules for such applications because they are easily synthesized, either by solid-phase chemical synthesis or by recombinant DNA technology, and self-assembly motifs can be based upon simple secondary structure elements such as α-helices (*9*) and β-sheets (*2*, *4*, *7*, *10*, *11*).

Previous work in our laboratory and others has focused upon peptides with alternating hydrophilic/hydrophobic primary structures that self-assemble into β-sheet fibrillar structures (*7*, *10*−*13*). At peptide concentrations in the 10−30 mM range, these fibrillar structures are sufficiently entangled to form gellike materials (*3*, *7*, *11*). These materials have recently been investigated as scaffolds for tissue engineering applications, and it has been found that they perform well as three-dimensional culture substrates for nerve cells (*2*) and chondrocytes (*3*). The propensity of these peptides to form β-sheet structures is conferred by their alternating primary structure, which positions all hydrophobic residues on one side of the β-sheet and all the hydrophilic residues on the other (*15*−*18*). Subsequent assembly into fibrillar structures then proceeds, in part by association of the hydrophobic faces of the β-sheets under solution conditions that effectively shield the electrostatic repulsive forces that arise from charged side-chains (*19*). That is, in aqueous salt solutions, self-assembly rapidly progresses, whereas self-assembly is retarded or absent in pure aqueous solutions (*12*). This salt-sensitivity has been utilized to develop materials that rapidly gel in response to certain triggers, such as body temperature or near-infrared light exposure (*7*).

Tailoring these assemblies by covalently attaching pendant biomolecules would be useful in several scenarios, including covalently attaching drugs or growth factors for controlled release (*20*−*22*) or for attaching peptides for ligand-specific interactions with cells (*23*−*25*). Recently, factor XIII, a transglutaminase enzyme, has been utilized by Hubbell and co-workers to covalently link cell-attachment peptides or heparin-binding peptides to self-assembled fibrin matrixes (*26*−*28*). Transglutaminases (TGases) catalyze the formation of isopeptide bonds between glutamine and lysine residues of proteins and polypeptides (Figure 1, for review see ref 29) and are attractive for covalent modification of self-assembled scaffolds because they operate under benign reaction conditions, have a high specificity, and can be triggered from an inactive to active form by the introduction of Ca^{2+} ions. In the work presented here, we developed a de novo self-assembling peptide as a scaffold for the subsequent attachment of other amine-containing biomolecules via tissue transglutaminase (tTGase) (Figure 2).

EXPERIMENTAL PROCEDURES

Chemicals. Except as noted below, all chemicals and reagents were purchased from Aldrich or Fisher and used as provided. Protected amino acids were purchased from Peptides International. Rink amide-AM resin and benzotriazol-1-yloxytripyrrolidinophosphonium hexafluorophosphate (PyBOP) were purchased from Nova Biochem. *N*-Methylpyrrolidone (NMP), *O*-benzotriazole-*N*,*N*,*N*′,*N*′-tetramethyluronium hexafluorophosphate (HBTU), 1-

* Corresponding author. Phone: 847-467-5273. Fax: 847-491-4928. E-mail: philm@northwestern.edu.

10.1021/bc034017t CCC: $25.00
Published on Web 06/24/2003

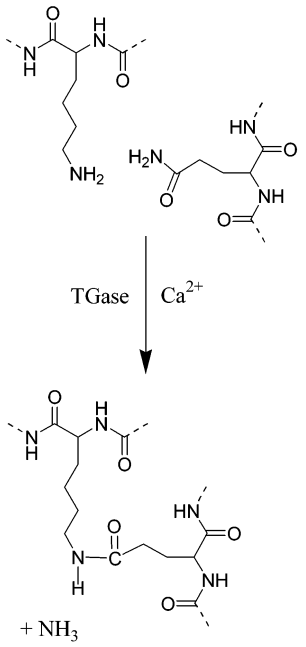

Figure 1. Transglutaminase-mediated coupling between lysine and glutamine residues.

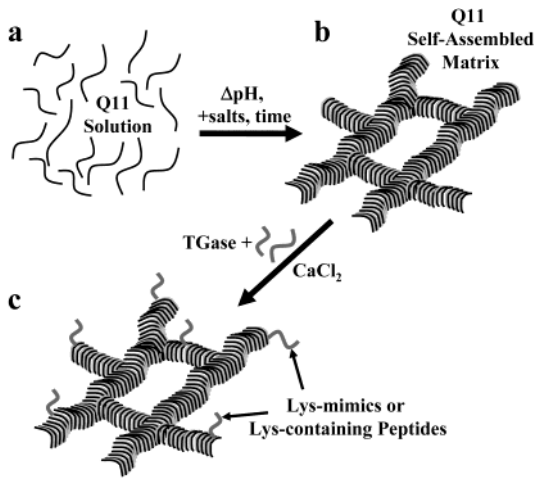

Figure 2. Schematic of Q11 self-assembly and subsequent modification by TGase. A Q11 solution (a) is induced to self-assemble, either by the addition of salts, a pH change, or the passage of time. The resultant self-assembled matrix (b) then serves as a tTGase substrate for the immobilization of appropriate lysine-containing biomolecules (c).

hydroxybenzotriazole (HOBt), *N*,*N*-diisopropylethylamine (DIEA), and piperidine were purchased from Applied Biosystems. All water was purified with a Barnstead-Thermolyne Nanopure Infinity water purifier to a resistivity of 18.1 MΩ-cm or greater.

Peptide Synthesis. Peptides Ac-QQKFQFQFEQQ-Am (Q11) and n-dansyl-GLKGGRGDS-Am (RGD1) were synthesized on a 0.25 mmol scale with standard fluorenylmethoxycarbonyl solid-phase techniques using an Applied Biosystems 433A automated peptide synthesizer. Rink amide resin (0.6 mmol/g substitution, 200−400 mesh) was used to produce C-terminal amides, activation was performed with 0.45M HOBt/HBTU in DMF (Fast-Moc kit, Applied Biosystems cat#401132), and coupling reactions were monitored with ninhydrin. RGD1 was dansylated by the incorporation of dansyl-Gly-OH at the N-terminus. Q11 was acetylated on-resin using 10 equiv of acetic acid, 10 equiv of HOBt, 10 equiv of PyBOP, and 20 equiv of DIEA in 5 mL NMP for 1 h. After being rinsed with NMP, dichloromethane (DCM), and 2-propanol, peptides were then cleaved from the resin and deprotected with 40 mL of 95% trifluoroacetic acid (TFA), 2.5% triisopropylsilane, and 2.5% water. After rotary evaporation of the cleavage cocktail to 3 mL, the peptides were precipitated and washed several times with cold ethyl ether. The cleaved peptides were then collected by centrifugation, dried overnight in vacuo, redissolved in water, lyophilized, and stored at −20 °C. The water solubility of lyophilized Q11 increased significantly after a second dissolution in TFA, precipitation from cold ether, resuspension in water, and re-lyophilization. It was presumed that this second dissolution in TFA enhanced Q11's water solubility by disaggregating any β-sheet aggregates (*30*). Identity of the peptides was confirmed with MALDI-TOF and ESI mass spectrometry. Q11 $[M + H]^+$ predicted *m*/*z*: 1527.69, observed: 1527.59. RGD1 $[M + H]^+$ predicted *m*/*z*: 1079.23, observed: 1079.20. Purity of peptides was estimated to be greater than 90% by HPLC (C4 reverse-phase column).

Self-Assembly and Secondary Structure Evaluation. To determine the solution conditions in which Q11 formed supramolecular aggregates, aqueous solutions of 2−30 mM Q11 were prepared. These solutions were then pipetted into either Dulbecco's phosphate-buffered saline (PBS), aqueous NaCl (1−100 mM), or aqueous $CaCl_2$ (1−100 mM). Each solution contained 10 μM Congo red, a dye that specifically binds β-sheet fibrillar aggregates (*31*). Alternatively, aqueous Q11 (2−30 mM) was pipetted onto the bottoms of multiwell dishes, allowed to dry, and then rehydrated with various solutions and buffers containing 10 μM Congo red. Congo red staining was then observed with brightfield microscopy and under cross-polarizers.

Circular dichroism (CD) and FTIR spectroscopy were utilized to evaluate the secondary structure characteristics of Q11. For CD, peptides were dissolved in water, and concentrations were verified spectrophotometrically by measuring the absorption of the phenylalanine residues at 260 nm (ϵ_{260} (Phe) = 187 M^{-1} cm^{-1}). pH was not adjusted for the CD concentration studies, and the pH was slightly acidic (pH 4.7), most likely from residual TFA. A stock solution of 1 mM Q11 was diluted to concentrations between 20 μM and 100 μM, and CD measurements were made within 20 min of dilution. Measurements were made on a JASCO J-715 from 190 to 280 nm with a 1 nm step resolution, a scan speed of 100 nm/min, 10 accumulations, a 10s response time, a 1 nm bandwidth, and data smoothing (3rd order, 7 point smoothing). Quartz cuvettes with a 10 mm path length were used. To study the effects of NaCl on the assembly of Q11 in dilute aqueous solutions, a stock solution of 1mM Q11 and a stock solution of 1mM NaCl were prepared. These were mixed and diluted with water to achieve a peptide concentration of 30 μM Q11 and 0−100 mM NaCl. CD measurements were then taken exactly 10 min after mixing.

FTIR spectroscopy was performed for concentrated Q11 (26 mM in 1:1 D_2O:H_2O) with a Biorad FTS-60 using a liquid cell with BaF_2 windows and 10 μm spacers. Q11 was water-soluble, but sparingly soluble in D_2O, so some precipitation was observed during analysis. Scans were performed between 1550 and 1750 cm^{-1} to monitor the amide I vibration. Sixteen scans were summed. For second-derivative calculations, the Savitsky−Golay method was used (2nd degree, 40−50 ponts).

Negative-Stained TEM and Quick-Freeze Deep-Etch (QFDE) TEM. To evaluate the self-assembled morphology of Q11, two electron microscopic techniques

were utilized. For negative staining, fibrils were allowed to form from concentrated aqueous Q11 solutions (40 mg/mL in water for 3 days under a layer of PBS). The PBS was then removed, and the formed fibrils were diluted 1:100 in H_2O, vortexed vigorously to disrupt the gellike self-assembled structure into small fragments, immediately applied to O_2 plasma-treated lacey carbon TEM grids, and stained with 1% uranyl acetate. Grids were then imaged directly on a JEOL JEM 1200-EX.

For QFDE TEM, Q11 was dissolved in water (40 mg/mL) and allowed to self-assemble for 3 days. The Q11 self-assembled structures were then rapidly frozen by slamming them against a copper block at −195 °C (Gentleman Jim device, Ted Pella, Inc., Irvine, CA). Fracture and deep etching were performed on a Cressington CFE 40. Fracture was performed at −186 °C, etching at −95 °C for 25 min, and replication at −125 °C with a ∼2 nm layer of PtC at a 20° angle followed by a strengthening coat of C at a 90° angle. TEM was performed on the replicas with a JEOL 120 CX.

Enzymatic Cross-Linking and Analysis. For enzymatic cross-linking studies, tTGase from guinea pig liver was used (Sigma T-5398). The substrate properties of Q11 in both early and mature states of self-assembly were investigated. tTGase was aliquotted at 1.2−3 units/mL in buffer containing 1.33 mM ethylenediaminetetraacetic acid (EDTA), 20 mM dithiothreitol, and 50 mM Tris (pH 7.4 at 37 °C). Aliquotting was performed on ice, and aliquots were stored at −80 °C until use. To evaluate the amine acceptor properties of Q11, the lysine-mimic monodansylcadaverine (MDC) was used. MDC is a convenient model molecule for TGase studies, as its sidechain mimics that of lysine, and it has been utilized extensively in investigations of TGases and their substrates (*32*−*35*).

To investigate the tTGase reactivity of freshly solublized Q11 in an early aggregation state (dilute Q11 solutions in water), aqueous solutions were prepared containing Q11 and MDC and immediately reacted with tTGase before any observable self-assembly had occurred. In a typical experiment, to a Q11 solution was added TGase, $CaCl_2$, and MDC (final concentrations: 0.1−1.5 mM Q11, 0.1−2 mM MDC, 1.67−2.0 mM $CaCl_2$, 0.4−1.0 U/mL TGase, and 50 mM Tris, pH 7.4−8). Control reactions lacked tTGase. These mixtures were then allowed to react for time periods from 2 min to several hours at either room temperature or at 37 °C. The reactions were quenched by the addition of TFA.

To study the tTGase reactivity of self-assembled Q11, Q11 was first self-assembled under the influence of dissolved ions and subsequently reacted via tTGase. In a typical experiment, Q11 was first dissolved in water at a concentration of 40 mg/mL (26 mM). Fifty microliyers of PBS was then layered over 10 μL of this Q11 solution to induce gelation. After 24 h of incubation at room temperature, the PBS layer was removed from the now gellike Q11 layer, and the self-assembled Q11 was reacted by adding tTGase, $CaCl_2$, and MDC (final concentrations: 1.35 U/mL tTGase, 2.8 mM $CaCl_2$, 1.35 mM MDC, 2.6 mM Q11, in self-assembled form, 45 mM Tris, pH 7.4 @ 37 °C). The mixture was vortexed vigorously to distribute the reactants among the self-assembled Q11 fibrils, and the reaction proceeded for 1 h at 37 °C. The Q11 fibrils were then collected by centrifugation. The reactions were quenched, and Q11 was disaggregated by the 10:1 dilution of the reacted fibrils in TFA. TFA addition solublized and disassembled the Q11 fibrils, producing nonviscous fluids. It is known that TFA is an excellent solvent for disaggregating these and similar β-sheet fibril-forming peptides (*30*), and disaggregated Q11 produced single peaks in reverse phase-HPLC. To investigate the suitability of peptide substrates for tTGase-mediated cross-linking to Q11, the peptide RGD1 was reacted with unassembled and self-assembled Q11 in the same manner as with MDC described above.

Reverse-Phase HPLC. To quantify the amount of MDC incorporation, a known quantity of an internal standard, dansyl-ϵ-aminocaproic acid, was dissolved in TFA and added to the TFA solutions containing disaggregated Q11 and its reaction products (dansyl-ϵ-aminocaproic acid standard curve $R^2 = 0.987$). These solutions were then analyzed on a Waters HPLC system equipped with a photodiode array detector and a Vydak analytical C4 reverse-phase column, in a 10%-63% acetonitrile gradient over 30 min. The amount of dansylated product was then calculated by comparing the areas of dansylated Q11 reaction product peaks with those of the dansyl-ϵ-aminocaproic acid internal standard peak at 280 nm. Absorbance of the dansyl groups at 280 nm was utilized for the peak measurements, as no other species present in the reaction mixtures absorbed at this wavelength. It was not possible to perform LC/MS experiments on these samples, as the TFA necessary to disaggregate the peptide gels confounds LC/MS analysis, but the HPLC chromatograms were compared with MALDI mass spectrometry data. The number of product peaks shown by HPLC corresponded to those observed with mass spectrometry, and it was assumed that the sequence of product peaks observed in HPLC corresponded to sequential additions of MDC (which are expected to be sequentially more hydrophobic with each MDC addition). Calculations of product concentrations then took into account the fact that Q11−MDC_x adducts had x times the dansyl fluorescence of singly labeled peptides.

Mass Spectrometry. To identify the tTGase-mediated cross-linking products of Q11, MALDI-TOF mass spectrometry was utilized (PE Biosystems Voyager DE-PRO System 6050). Quenched enzyme reactions were mixed 1:1 with a solution of saturated α-cyano-4-hydroxycinnamic acid (CHCA) in 1:1 acetonitrile:H_2O with 0.1%TFA. These mixtures were then spotted onto a 100-well MALDI plate and dried in ambient conditions. Peptides and peptide conjugates were analyzed both in positive and negative reflector mode with delayed extraction, typically with an accelerating voltage of 25 kV, a grid voltage of 75%, a mirror voltage ratio of 1.12, a guide wire voltage of 0.05%, and a delay time of 360 ns. Scans were averaged over 100 laser shots, and spectra were baseline-corrected and noise-filtered.

RESULTS

Q11 Self-Assembles in Aqueous Solutions. Q11 was observed to have a high solubility in water, up to 50 mg/mL. Interestingly, it was observed that this solubility sometimes decreased upon extended storage as a lyophilized powder at −20 °C, but that maximal water solubility of the peptide could be restored by dissolving Q11 in TFA, precipitating in Et_2O, and re-lyophilizing. It is suspected that this TFA treatment disaggregates β-sheet structures that render the peptide insoluble (*30*). From its water-soluble state, Q11 self-assembled into gellike materials in a variety of aqueous solutions. For example, Q11 rapidly formed Congo-red stainable structures in 1−100 mM NaCl, 1−100 mM $CaCl_2$, and PBS (Figure 3). Also, when Q11 was incubated in concentrations from 10 to 30 mM in pure water at room temperature for time

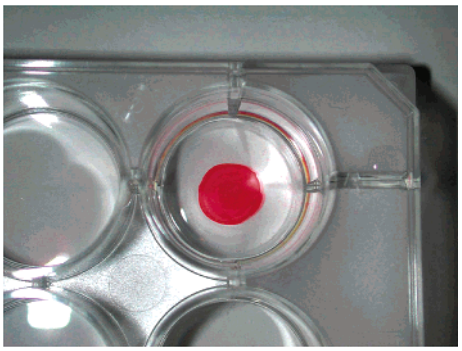

Figure 3. Congo red-stained Q11 in a 12-well polystyrene culture dish. An aqueous solution of 40 mg/mL Q11 was pipetted onto the bottom of the dish, dried in a fume hood, and then rehydrated with Dulbecco's PBS containing 30 μM Congo red. The staining solution was removed after 3 days and replaced with fresh PBS.

periods on the order of a few days, gellike materials were produced. This indicates that Q11 also self-assembles in pure water, albeit more slowly than in salt-containing solutions. Under cross-polarizers, Congo red-stained peptide aggregates possessed the characteristic apple-green birefringence that is a hallmark of Congo red-stained β-sheet fibrils (*31*).

Q11 Forms a Predominantly β-Sheet Secondary Structure. Using CD and FTIR spectroscopy, the secondary structure of Q11 was evaluated. CD spectra of very dilute solutions of Q11 (20−30 μM) resembled those expected for unordered peptide conformations (*36*, *37*). However, increasing the concentration of Q11 induced a conformational change to a structure that resembles an aggregated β-sheet (Figure 4a). The developing negative peak near 220 nm is a hallmark of β-sheet conformation (*37*). The addition of NaCl to dilute Q11 solutions (30 μM) also induced a conformational change from a random coil to a conformation resembling an aggregated β-sheet (Figure 4b). This behavior of β-sheet formation in a salt- and concentration-dependent manner is consistent with other similar short β-sheet forming peptides (*7*, *10*, *12*, *19*). FTIR spectra further supported that Q11 forms β-sheet secondary structures above the 0.1mM regime and in the presence of salts. For concentrated Q11 solutions (40 mg/mL in 1:1 D_2O:H_2O), major absorbances were seen at 1620 cm^{-1} and 1692 cm^{-1} (antiparallel β-sheet), and minor absorbances were seen at 1653 cm^{-1} (helix) and 1672 (residual TFA) (Figure 5) (*38*). For Q11 in salt-containing solutions (40 mg/mL Q11 in 50 mM $CaCl_2$, 1:1 D_2O:H_2O), major absorbances were seen at 1619 cm^{-1} and 1692 cm^{-1} (antiparallel β-sheet), and minor absorbances were seen at 1654 cm^{-1} (helix) and 1672 cm^{-1} (residual TFA) (data not shown). This indicates that while there is a small amount of helical structure, β-sheet structure predominates in concentrated Q11 solutions, both in the presence of salts and in pure aqueous solutions. Furthermore, these IR absorbances are similar to other previously studied β-sheet fibril-forming peptides (*7*).

Electron Microscopy of Self-Assembled Nanostructures. Quick-freeze deep etch (QFDE) TEM indicated that the self-assembly product of Q11 is a loosely entangled network of fibrils (Figure 6a). In QFDE images, fibril widths were on average about 20 nm, and the distance between entanglement points appeared to be about 100 nm. Uranyl acetate staining of fibrils that had been dried onto TEM grids showed that the structure of self-assembled Q11 appears to be a network of individual fibrils with widths of 4−8 nm (Figure 6b). Lateral

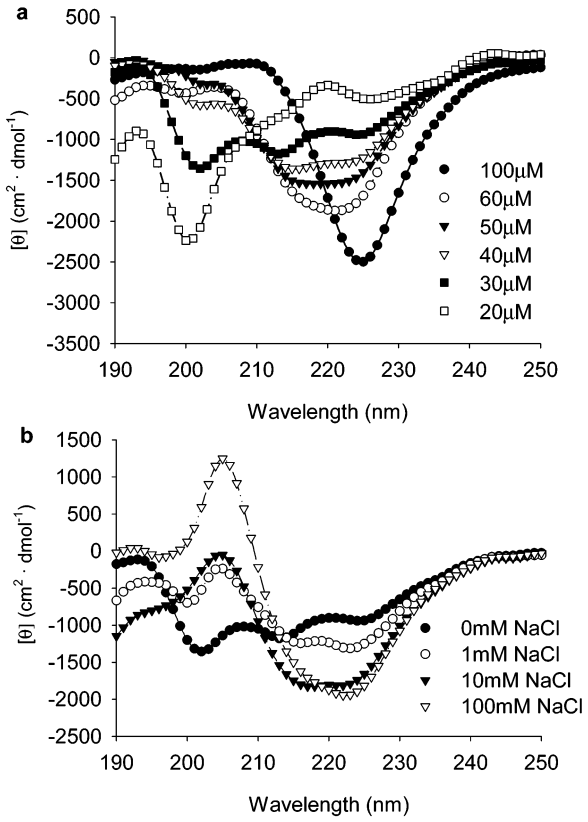

Figure 4. Circular Dichroism of Q11 in dilute solutions. Q11 in a range of concentrations in water (a) showed a conformational switch from an unordered conformation at low concentrations (20−30 μM) to increasing amounts of β-sheet content above concentrations of 40 μM. A similar transition can be induced in 30 μM Q11 by the addition of salts, such as NaCl (b).

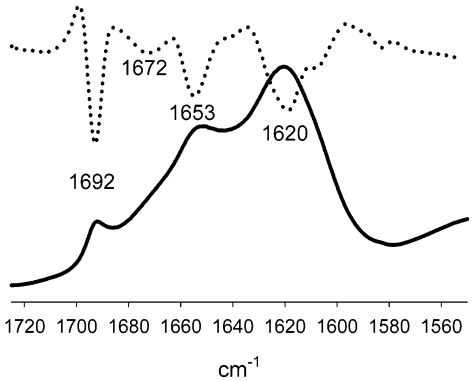

Figure 5. FTIR spectrum (solid) and second-derivative (dotted) for Q11, 40 mg/mL in 1:1 H_2O:D_2O. Major peaks at 1620 cm^{-1} and 1692 cm^{-1} indicate that Q11 is predominantly in a β-sheet structure, and the smaller peak at 1653 cm^{-1} indicates that some helical structure is also present. The small absorbance at 1672 cm^{-1} is a result of trace amounts of TFA.

association of these fibrils was also observed, in some cases forming cables with overall widths of 15−30 nm. This self-assembled morphology is similar to that of several other well-known β-sheet fibril-forming peptides and proteins. For example, amyloids formed from a wide variety of natural peptides form fibrils of remarkably similar structure (*39*). Also, the alternating hydrophobic−hydrophilic peptides studied by Zhang and co-workers form similar 10−20 nm wide fibrils in loosely entangled networks (*2*, *12*). Furthermore, other alternating peptides have been observed to first self-assemble into ~8 nm wide fibrils and subsequently aggregate into thicker bands of parallel fibrils (*40*).

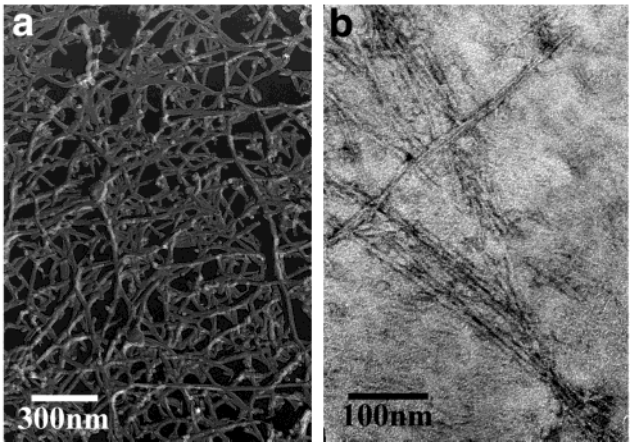

Figure 6. QFDE (a) and negative stained (b) TEM images. QFDE showed that Q11 self-assembles into a highly entangled network of fibrils, with ~20 nm diameter fibrils and ~100 nm between entanglement points. Negative staining revealed smaller fibrils, about 8 nm in diameter, in entangled networks.

MALDI-TOF Mass Spectrometry. MALDI-TOF mass spectrometry was utilized to investigate the tTGase substrate properties of Q11 because other analysis techniques (such as gel electrophoresis) were hindered by the tendency of Q11 to aggregate in buffers, even in the presence of high concentrations of denaturing agents such as SDS, urea, or guanidinium chloride. In contrast, MALDI-TOF mass spectrometry accurately identified peptides and cross-linked species. Furthermore, because mass spectrometry has a much finer resolution (<1 Da) than electrophoresis, the NH_3 evolution that is a property of TGase cross-linking (Figure 1) was utilized as verification that the products observed were in fact tTGase-mediated cross-linking products rather than noncovalent aggregates. The substrate properties of Q11 were first evaluated with monodansylcadaverine (MDC), a lysine mimic that has been extensively utilized for the investigation of TGases and their substrates (*32*−*35*). With its lysine-mimicking side chain and dansyl fluorophore, MDC is a convenient label for identifying tTGase-mediated reaction products with mass spectrometry and UV spectrophotometry. After reaction of Q11 with tTGase in dilute solutions (below the concentration required to produce macroscopic gels), mass spectra showed the emergence of product peaks with *m/z* values corresponding to Q11−MDC adducts with up to four attached MDC molecules (Figure 7a). Strong positive *m/z* peaks were observed for unreacted Q11, $[Q11 + H]^+$ calcd: 1527.69, observed: 1527.59 and the Q11−MDC adducts (subtracting the mass of one NH_3 per couple) $[Q11 + MDC + H]^+$ calcd: 1846.08, observed: 1846.77; $[Q11 + 2MDC + H]^+$ calcd: 2164.48, observed: 2164.91; $[Q11 + 3MDC + H]^+$ calcd: 2482.87, observed: 2483.11; and $[Q11 + 4MDC + H]^+$ calcd: 2801.27 observed: 2801.23. Control experiments (without tTGase) showed no evolution of any product peaks.

For Q11 that had self-assembled into a gellike material under the influence of salt ions, mass spectrometry showed that up to five glutamines were active, as there existed Q11 peptides with as many as five conjugated MDC molecules after 1 h of reaction (Figure 7b). In these mass spectra, most species were observed to be associated with one and sometimes two Na^+ ions (22.99 Da), a result of using PBS to self-assemble the Q11 before tTGase reaction (Figure 7b, inset). Strong positive *m/z* peaks were observed for unreacted Q11, $[Q11 + Na]^+$ calcd: 1549.67, observed: 1549.27 and the Q11−MDC adducts

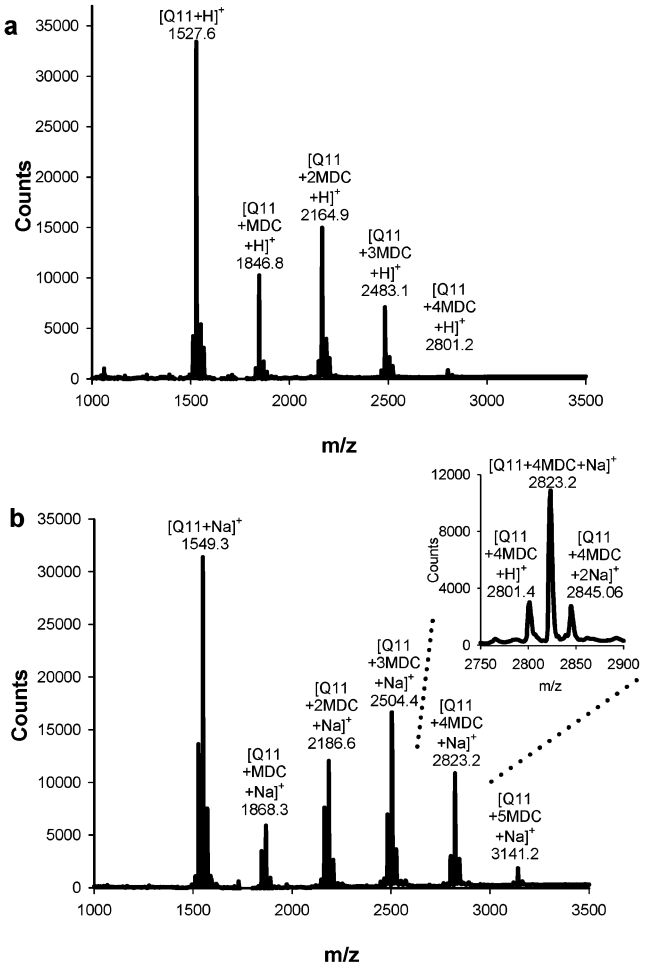

Figure 7. MALDI-TOF MS spectra of tTGase-mediated cross-linking reactions. (a) Soluble Q11 and MDC (reaction conditions: 1 U/mL tTGase, 2 mM $CaCl_2$, 1 mM MDC, 1 mM Q11 (unassembled, freshly dissolved), in 33.3 mM Tris, pH 7.4, for 1 h at 37 °C). (b) Self-assembled Q11 and MDC (reaction conditions: 1.35 U/mL tTGase, 2.81 mM $CaCl_2$, 1.35 mM MDC, 2.62 mM Q11 (previously assembled under a layer of PBS), 45 mM Tris, pH 7.4 for 1 h at 37 °C. For Q11 that had been self-assembled under a layer of PBS, Na^+ adducts were observed (b, inset).

(subtracting the mass of one NH_3 per couple) $[Q11 + MDC + Na]^+$ calcd: 1868.06, observed: 1868.24; $[Q11 + 2MDC + Na]^+$ calcd: 2186.46, observed: 2186.65; $[Q11 + 3MDC + Na]^+$ calcd: 2504.85, observed: 2504.44; $[Q11 + 4MDC + Na]^+$ calcd: 2823.25, observed: 2823.21; and $[Q11 + 5MDC + Na]^+$ calcd: 3141.64, observed: 3141.18. These data clearly show that MDC is covalently coupled to the self-assembled Q11 at as many as five glutamine locations via tTGase.

MALDI-TOF mass spectrometry also showed that tTGase could be utilized to conjugate the bidomain peptide RGD1 to Q11. This peptide was designed such that the N-terminal end possessed a Leu-Lys sequence for tTGase substrate activity (*41*). The C-terminal end possessed an integrin-binding RGD sequence for future cell-attachment studies, and a diglycinyl spacer separated the two domains. MALDI showed that up to five RGD1 peptides could be coupled to Q11 via transglutaminase in 1 h (Figure 8). Strong positive *m/z* peaks were observed for unreacted Q11, $[Q11 + H]^+$ calcd: 1527.7, observed: 1527.3; unreacted RGD1, $[RGD1 + H]^+$ calcd: 1079.2, observed: 1079.2 and the Q11−RGD1 adducts (subtracting the mass of one NH_3 per couple) $[Q11 + RGD1 + H]^+$ calcd: 2588.8, observed: 2589.2; $[Q11 + 2RGD1 + H]^+$

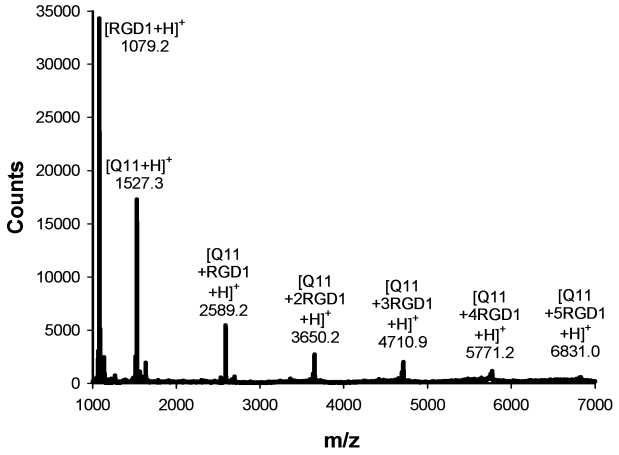

Figure 8. MALDI-TOF MS spectrum of TGase-mediated cross-linking reactions between Q11 and RGD1 peptides. Reaction conditions: 0.4 U/mL tTGase, 1.67 mM $CaCl_2$, 1 mM RGD1, 0.25 mM Q11 (unassembled, freshly dissolved), in 50 mM Tris, pH 7.4 at 37 °C for 70 min).

Table 1. Quantification of Q11−MDC Cross-linking Products for Soluble and Self-Assembled Q11 (mean ± one standard deviation).

product	soluble Q11[a] (% of total Q11)	self-assembled Q11[b] (% of total Q11)
unconjugated Q11	85.5% ± 2.1%	93.7% ± 2.5%
Q11 + 1MDC	4.9% ± 0.67%	2.6% ± 0.9%
Q11 + 2MDC	4.0% ± 0.58%	1.7% ± 0.7%
Q11 + 3MDC	2.8% ± 0.57%	1.0% ± 0.4%
Q11 + 4MDC	2.2% ± 0.8%	0.7% ± 0.3%
Q11 + 5MDC	0.6% ± 0.23%	0.2% ± 0.07%

[a] Reaction conditions: 1 U/mL tTGase, 2 mM $CaCl_2$, 1 mM MDC, 1 mM Q11 (unassembled, freshly dissolved), in 33.3 mM Tris, pH 7.4, for 1 h at 37 °C. [b] Reaction conditions: 1.35 U/mL tTGase, 2.81 mM $CaCl_2$, 1.35 mM MDC, 2.62 mM Q11 (previously assembled under a layer of PBS), 45 mM Tris, pH 7.4 for 1 h at 37 °C.

calcd: 3649.9, observed: 3650.2; $[Q11 + 3RGD1 + H]^+$ calcd: 4711.0, observed: 4710.9; $[Q11 + 4RGD1 + H]^+$ calcd: 5772.1, observed: 5771.2; and $[Q11 + 5RGD1 + H]^+$ calcd: 6833.3, observed: 6831.0. These results indicate that lysine-containing peptides can be coupled to Q11 in the same way that MDC can be coupled.

HPLC Quantification of Q11−MDC Cross-Linking. Because the quantification of reaction products is difficult with MALDI due to the sensitivity of peak height to instrument parameters and ionization efficiencies, HPLC was utilized to quantify the tTGase-mediated cross-linking products between Q11 and the model lysine-mimic MDC. Chromatograms were collected at 280 nm (dansyl) and 215 nm (amide). Only product peaks (with their conjugated dansyl groups from MDC) absorbed at 280 nm, and their concentrations were calculated by comparing their peak areas at 280 nm to the area of the dansyl-ϵ-aminocaproic acid internal standard peak. The amount of each reaction product was then expressed as a percentage of total Q11 available in the original reaction mixture. HPLC analysis showed that in dilute reaction conditions, the amount of Q11 peptides that were conjugated to at least one MDC molecule was on average 14.5% at 1 h of reaction time. The distribution of Q11 reaction products is listed in Table 1. From these data it can be seen that Q11 with one conjugated MDC is the most common product, with each subsequent MDC addition occurring less frequently. For self-assembled Q11, HPLC showed that on average up to 6.3% of the available Q11 was coupled to at least one MDC molecule, with five

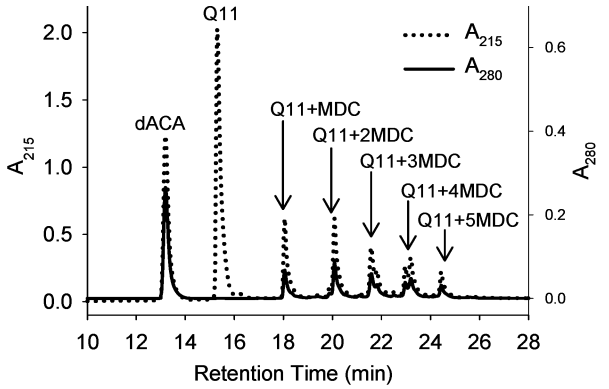

Figure 9. HPLC quantification of tTGase-mediated cross-linking between self-assembled Q11 and MDC. Quantities of reaction products are listed in Table 1.

product peaks observed (Figure 9). The quantities of each product are shown in Table 1. Again, Q11 with one grafted MDC is the most common product, with each subsequent MDC addition occurring less frequently. The reaction conditions for the data shown in Figure 9 and in Table 1 are the same as those described for the Q11−MDC cross-linking reactions that were analyzed by mass spectrometry (Figure 7). The reaction conditions varied slightly between the experiments performed on unassembled Q11 and self-assembled Q11 (for both the MALDI and HPLC experiments), so differences in substrate properties between self-assembled and unassembled Q11 are not easily made from these data. However, it is clear that MDC can be coupled in significant amounts to both unassembled and self-assembled Q11 via tTGase.

DISCUSSION

To produce a short peptide that both self-assembles into β-sheet fibrillar structures and acts as a transglutaminase substrate, a number of natural and synthetic peptides were considered. Common features between these peptides were then incorporated into the design of Q11. For example, a water-soluble peptide designed by Aggeli and co-workers (*10*, *42*), Ac-QQRFQWQFEQQ-Am (DN1), self-assembles into β-sheet fibrillar structures and has a high content of glutamine residues for possible TGase reactivity. Another peptide that possesses these properties is a sequence from an extracellular matrix protein, microfibril-associated glycoprotein-1 (MAGP-1, residues 57−80, PPEEQFQFQSQQQVQQEVIPAPTL) (*43*). This fragment, possessing an alternating QFQFQ central sequence and many Gln residues, self-assembles into Congo-red stainable β-sheet structures. Interestingly, MAGP-1 is a transglutaminase substrate, though it is not yet known whether the glutamines within this β-sheet-forming domain are active (*43*). In other work involving alternating hydrophilic−hydrophobic peptides (which have a high propensity for forming β-sheet structures), Caplan and co-workers designed a β-sheet fibril-forming peptide, FKFQFKFQFKFQ, from alternating glutamine, lysine, and phenylalanine residues (*44*, *45*). Last, amyloidogenic peptides such as polyglutamines and the Alzheimers peptide Aβ are well-known β-sheet fibril formers and can also act as transglutaminase substrates (*46*−*48*). Longer polyglutamines, however, are key pathological components of neurodegenerative disorders such as Huntington's disease, in which polyglutamines of 30−100 Gln residues (depending on severity of the disease) show a toxic gain of function (*49*). Aβ is also a key pathological component

in Alzheimer's disease, though its specific role remains elusive (*39*, *50*). As such, these potentially toxic natural peptides would be inappropriate for potential biomedical applications, but short, nontoxic Gln repeats still possess TGase reactivity (*46*). Thus, the peptide described here, Q11, Ac-QQKFQFQFEQQ-Am, possesses key features of the peptides mentioned above, having 11 amino acids in an overall layout similar to Aggeli et al.'s DN1, an alternating FQFQF core, and short polyglutamine repeats. Furthermore, it is neutrally charged to avoid electrostatic repulsion in self-assembly.

It is interesting that Q11 was not found to be both an acyl acceptor (lysine substrate), as well as an acyl donor (glutamine substrate). Although Q11 possesses one potentially active lysine residue, experiments performed to specifically look for this cross-linking reaction showed no evidence of Q11−Q11 conjugation (data not shown). This result is particularly interesting because it is widely considered that the sequence specificity of tTGase is less stringent for amines than for glutamine residues (*51*). Perhaps Lys_3 in Q11 is buried within the β-sheet fibril in such a way as to render it inaccessible to the enzyme. It would be interesting to develop a β-sheet fibril-forming peptide that can be cross-linked to itself in a "covalent capture" approach (*5*, *52*). In such a strategy, the strength or stiffness of the self-assembled matrix could be increased via the generation of intermolecular cross-links. Another interesting result was that both the self-assembled and unassembled Q11 possessed similar tTGase substrate characteristics. This could be because the "unassembled" Q11, even when freshly dissolved in low concentrations, most likely exists in some early state of self-assembly and not truly in a unimolecular state in solution. The CD data shows that even in the micromolar regime, Q11 exists in a β-sheet conformation, even without the presence of salts. This suggests that the Q11 is self-associating, at least into bimolecular or oligomolecular aggregates, as it is possible but unlikely that the Q11 adopts a unimolecular β-sheet conformation.

The potential utility of this approach includes applications in drug delivery, in tissue engineering, and as tissue glues. Recent investigations have focused on similar β-sheet fibril-forming peptides for tissue engineering (*2*, *3*), demonstrating that similar β-sheet fibril forming peptides appear to be nonimmunogenic (*2*) and are able to support the three-dimensional culture of chondrocytes (*3*) as well as nerve cells (*2*). Also, earlier studies showed that similar self-assembled scaffolds supported the culture of a wide variety of cell types (*4*). The approach presented here for tTGase-mediated decoration of these self-assembled scaffolds could lead to the tailoring such matrixes for the presentation of appropriate cell-binding ligands (*27*, *28*) or even growth factors (*26*) to induce desired cellular functions. As a proof-of-concept, we have shown that fusion peptides of tTGase substrates and bioactive sequences (such as the integrin-binding RGD sequence) can be coupled to Q11 scaffolds with tTGase. Ongoing studies in our laboratory are investigating whether cell attachment to Q11 scaffolds can be modulated by the tTGase-mediated grafting of integrin-binding peptides to Q11.

CONCLUSIONS

An 11-amino acid peptide, Q11, was synthesized and observed to self-assemble into β-sheet fibrillar structures. This peptide was also able to covalently couple to lysine mimics and lysine-containing peptides via tissue transglutaminase. This approach is potentially useful for the covalent modification of self-assembling peptide systems for biomedical applications.

ACKNOWLEDGMENT

We would like to thank Annelise Barron for use of the peptide synthesizer, Jiahn-Dar Huang for processing the QFDE samples, and Bi-Huang Hu for helpful discussions regarding peptide synthesis and characterization. This work was funded by NIH grants R01 DE 13030 and T32 DE 07042.

Supporting Information Available: HPLC chromatogram and MALDI-TOF mass spectrum of Q11. This material is available free of charge via the Internet at http://pubs.acs.org.

LITERATURE CITED

(1) Holmes, T. C. (2002) Novel peptide-based biomaterial scaffolds for tissue engineering. *Trends Biotechnol. 20*, 16−21.

(2) Holmes, T. C., de Lacalle, S., Su, X., Liu, G. S., Rich, A., and Zhang, S. G. (2000) Extensive neurite outgrowth and active synapse formation on self-assembling peptide scaffolds. *Proc. Nat. Acad. Sci. U.S.A. 97*, 6728−6733.

(3) Kisiday, J., Jin, M., Kurz, B., Hung, H., Semino, C., Zhang, S., and Grodzinsky, A. J. (2002) Self-assembling peptide hydrogel fosters chondrocyte extracellular matrix production and cell division: Implications for cartilage tissue repair. *Proc. Nat. Acad. Sci. U.S.A. 99*, 9996−10001.

(4) Zhang, S. G., Holmes, T. C., DiPersio, C. M., Hynes, R. O., Su, X., and Rich, A. (1995) Self-complementary oligopeptide matrices support mammalian cell attachment. *Biomaterials 16*, 1385−1393.

(5) Hartgerink, J. D., Beniash, E., and Stupp, S. I. (2001) Self-assembly and mineralization of peptide-amphiphile nanofibers. *Science 294*, 1684−1688.

(6) Fields, G. B., Lauer, J. L., Dori, Y., Forns, P., Yu, Y. C., and Tirrell, M. (1998) Proteinlike molecular architecture: Biomaterial applications for inducing cellular receptor binding and signal transduction. *Biopolymers 47*, 143−151.

(7) Collier, J. H., Hu, B. H., Ruberti, J. W., Zhang, J., Shum, P., Thompson, D. H., and Messersmith, P. B. (2001) Thermally and photochemically triggered self-assembly of peptide hydrogels. *J. Am. Chem. Soc. 123*, 9463−9464.

(8) Caplan, M. R., and Lauffenburger, D. A. (2002) Nature's complex copolymers: Engineering design of oligopeptide materials. *Ind. Eng. Chem. Res. 41*, 403−412.

(9) Petka, W. A., Harden, J. L., McGrath, K. P., Wirtz, D., and Tirrell, D. A. (1998) Reversible hydrogels from self-assembling artificial proteins. *Science 281*, 389−392.

(10) Aggeli, A., Bell, M., Boden, N., Keen, J. N., Knowles, P. F., McLeish, T. C. B., Pitkeathly, M., and Radford, S. E. (1997) Responsive gels formed by the spontaneous self-assembly of peptides into polymeric beta-sheet tapes. *Nature 386*, 259−262.

(11) Schneider, J. P., Pochan, D. J., Ozbas, B., Rajagopal, K., Pakstis, L., and Kretsinger, J. (2002) Responsive hydrogels from the intramolecular folding and self-assembly of a designed peptide. *J. Am. Chem. Soc. 124* 15030−15037.

(12) Zhang, S. G., Holmes, T., Lockshin, C., and Rich, A. (1993) Spontaneous assembly of a self-complementary oligopeptide to form a stable macroscopic membrane. *Proc. Nat. Acad. Sci. U.S.A. 90*, 3334−3338.

(13) Lashuel, H. A., LaBrenz, S. R., Woo, L., Serpell, L. C., and Kelly, J. W. (2000) Protofilaments, filaments, ribbons, and fibrils from peptidomimetic self-assembly: Implications for amyloid formation and materials science. *J. Am. Chem. Soc. 122*, 5262−5277.

(14) MacPhee, C. E., and Dobson, C. M. (2000) Formation of mixed fibrils demonstrates the generic nature and potential utility of amyloid nanostructures. *J. Am. Chem. Soc. 122*, 12707−12713.

(15) West, M. W., Wang, W. X., Patterson, J., Mancias, J. D., Beasley, J. R., and Hecht, M. H. (1999) De novo amyloid

proteins from designed combinatorial libraries. *Proc. Nat. Acad. Sci. U.S.A. 96*, 11211−11216.
(16) West, M. W., and Hecht, M. H. (1995) Binary patterning of polar and nonpolar amino acids in the sequences and structures of native proteins. *Protein Sci. 4*, 2032−2039.
(17) Brack, A., and Orgel, L. E. (1975) Beta structures of alternating polypeptides and their possible prebiotic significance. *Nature 256*, 383−387.
(18) Xiong, H. Y., Buckwalter, B. L., Shieh, H. M., and Hecht, M. H. (1995) Periodicity of Polar and Nonpolar Amino-Acids Is the Major Determinant of Secondary Structure in Self-Assembling Oligomeric Peptides. *Proc. Nat. Acad. Sci. U.S.A. 92*, 6349−6353.
(19) Caplan, M. R., Moore, P. N., Zhang, S., Kamm, R. D., and Lauffenburger, D. A. (2000) Self-assembly of a beta-sheet protein governed by relief of electrostatic repulsion relative to van der Waals attraction. *Biomacromolecules 1*, 627−631.
(20) Mann, B. K., Schmedlen, R. H., and West, J. L. (2001) Tethered-TGF-beta increases extracellular matrix production of vascular smooth muscle cells. *Biomaterials 22*, 439−444.
(21) Kuhl, P. R., and Griffith-Cima, L. G. (1996) Tethered epidermal growth factor as a paradigm for growth factor-induced stimulation from the solid phase. *Nat. Med. 2*, 1022−1027.
(22) Bentz, H., Schroeder, J. A., and Estridge, T. D. (1998) Improved local delivery of TGF-beta 2 by binding to injectable fibrillar collagen via difunctional polyethylene glycol. *J. Biomed. Mater. Res. 39*, 539−548.
(23) Hubbell, J. A., Massia, S. P., Desai, N. P., and Drumheller, P. D. (1991) Endothelial Cell-Selective Materials for Tissue Engineering in the Vascular Graft Via a New Receptor. *Bio/Technology 9*, 568−572.
(24) Massia, S. P., and Hubbell, J. A. (1990) Covalently Attached GRGD on Polymer Surfaces Promotes Biospecific Adhesion of Mammalian-Cells. *Ann. N. Y. Acad. Sci. 589*, 261−270.
(25) Cook, A. D., Hrkach, J. S., Gao, N. N., Johnson, I. M., Pajvani, U. B., Cannizzaro, S. M., and Langer, R. (1997) Characterization and development of RGD-peptide-modified poly(lactic acid-*co*-lysine) as an interactive, resorbable biomaterial. *J. Biomed. Mater. Res. 35*, 513−523.
(26) Sakiyama-Elbert, S. E., and Hubbell, J. A. (2000) Development of fibrin derivatives for controlled release of heparin-binding growth factors. *J. Controlled Release 65*, 389−402.
(27) Schense, J. C., and Hubbell, J. A. (1999) Cross-linking exogenous bifunctional peptides into fibrin gels with factor XIIIa. *Bioconjugate Chem. 10*, 75−81.
(28) Schense, J. C., and Hubbell, J. A. (2000) Three-dimensional migration of neurites is mediated by adhesion site density and affinity. *J. Biol. Chem. 275*, 6813−6818.
(29) Lorand, L., and Conrad, S. M. (1984) Transglutaminases. *Mol. Cell Biochem. 58*, 9−35.
(30) Jao, S. C., Ma, K., Talafous, J., Orlando, R., and Zagorski, M. G. (1997) Trifluoroacetic acid pretreatment reproducibly disaggregates the amyloid beta-peptide. *Amyloid 4*, 240−252.
(31) Pears, A. G. E. (1960) Histochemistry: Theoretical and Applied, Little, Brown, Boston.
(32) Lorand, L., Siefring, G. E., Tong, Y. S., Brunerlorand, J., and Gray, A. J. (1979) Dansylcadaverine Specific Staining for Transamidating Enzymes. *Anal. Biochem. 93*, 453−458.
(33) Jeitner, T. M., Fuchsbauer, H. L., Blass, J. P., and Cooper, A. J. L. (2001) A sensitive fluorometric assay for tissue transglutaminase. *Anal. Biochem. 292*, 198−206.
(34) Zhang, Z. Y., Shum, P., Yates, M., Messersmith, P. B., and Thompson, D. H. (2002) Formation of fibrinogen-based hydrogels using phototriggerable diplasmalogen liposomes. *Bioconjugate Chem. 13*, 640−646.
(35) Valnickova, Z., and Enghild, J. J. (1998) Human procarboxypeptidase U, or thrombin-activable fibrinolysis inhibitor, is a substrate for transglutaminases − Evidence for transglutaminase-catalyzed cross-linking to fibrin. *J. Biol. Chem. 273*, 27220−27224.
(36) Johnson, W. C. (1988) Secondary structure of proteins through circular dichroism spectroscopy. *Annu. Rev. Biophys. Biophys. Chem. 17*, 145−166.
(37) Greenfield, N., and Fasman, G. D. (1969) Computed Circular Dichroism Spectra for Evaluation of Protein Conformation. *Biochemistry 8*, 4108−4116.
(38) Haris, P. I., and Chapman, D. (1995) The conformational analysis of peptides using Fourier transform IR spectroscopy. *Biopolymers 37*, 251−263.
(39) Lynn, D. G., and Meredith, S. C. (2000) Review: Model peptides and the physicochemical approach to beta-amyloids. *J. Struct. Biol. 130*, 153−173.
(40) Marini, D. M., Hwang, W., Lauffenburger, D. A., Zhang, S. G., and Kamm, R. D. (2002) Left-handed helical ribbon intermediates in the self-assembly of a beta-sheet peptide. *Nano Lett. 2*, 295−299.
(41) Gross, M., Whetzel, N. K., and Folk, J. E. (1977) Amine Binding-Sites in Acyl Intermediates of Transglutaminases − Human-Blood Plasma Enzyme (Activated Coagulation Factor-XIII) and Guinea-Pig Liver-Enzyme. *J. Biol. Chem. 252*, 3752−3759.
(42) Aggeli, A., Bell, M., Boden, N., Keen, J. N., McLeish, T. C. B., Nyrkova, I., Radford, S. E., and Semenov, A. (1997) Engineering of peptide beta-sheet nanotapes. *J. Mater. Chem. 7*, 1135−1145.
(43) Trask, B. C., Broekelmann, T., Ritty, T. M., Trask, T. M., Tisdale, C., and Mecham, R. P. (2001) Posttranslational modifications of microfibril associated glycoprotein- 1 (MAGP-1). *Biochemistry 40*, 4372−80.
(44) Caplan, M. R., Schwartzfarb, E. M., Zhang, S. G., Kamm, R. D., and Lauffenburger, D. A. (2002) Effects of systematic variation of amino acid sequence on the mechanical properties of a self-assembling, oligopeptide biomaterial. *J. Biomater. Sci. Polym. Ed. 13*, 225−236.
(45) Caplan, M. R., Schwartzfarb, E. M., Zhang, S. G., Kamm, R. D., and Lauffenburger, D. A. (2002) Control of self-assembling oligopeptide matrix formation through systematic variation of amino acid sequence. *Biomaterials 23*, 219−227.
(46) Kahlem, P., Terre, C., Green, H., and Djian, P. (1996) Peptides containing glutamine repeats as substrates for transglutaminase-catalyzed cross-linking: relevance to diseases of the nervous system. *Proc. Nat. Acad. Sci. U.S.A. 93*, 14580−5.
(47) Benzinger, T. L. S., Gregory, D. M., Burkoth, T. S., Miller-Auer, H., Lynn, D. G., Botto, R. E., and Meredith, S. C. (1998) Propagating structure of Alzheimer's beta-amyloid(10−35) is parallel beta-sheet with residues in exact register. *Proc. Nat. Acad. Sci. U.S.A. 95*, 13407−12.
(48) Dudek, S. M., and Johnson, G. V. W. (1994) Transglutaminase Facilitates the Formation of Polymers of the Beta-Amyloid Peptide. *Brain Res. 651*, 129−133.
(49) Zoghbi, H. Y., and Orr, H. T. (2000) Glutamine repeats and neurodegeneration. *Annu. Rev. Neurosci. 23*, 217−47.
(50) Koo, E. H., Lansbury, P. T., and Kelly, J. W. (1999) Amyloid diseases: abnormal protein aggregation in neurodegeneration. *Proc. Nat. Acad. Sci. U.S.A. 96*, 9989−90.
(51) Greenberg, C. S., Birckbichler, P. J., and Rice, R. H. (1991) Transglutaminases − Multifunctional Cross-Linking Enzymes That Stabilize Tissues. *FASEB J. 5*, 3071−3077.
(52) Clark, T. D., Kobayashi, K., and Ghadiri, M. R. (1999) Covalent capture and stabilization of cylindrical β-sheet peptide assemblies. *Chem. Eur. J. 5*, 782−792.

BC034017T